

# Effect of Rolling and Post-Annealing on the Microstructure and Properties of Explosively Welded Al/Cu Joints

H. Jamali<sup>1</sup>, K. Khajavi<sup>1</sup>, M. R. Khanzadeh<sup>1,\*</sup>, K. Amini<sup>2</sup>, H. Bakhtiari<sup>3</sup>

<sup>1</sup>Department of Materials Engineering, Mo.C., Islamic Azad University, Isfahan, Iran.

<sup>2</sup>Department of Mechanical Engineering, Kho.C., Islamic Azad University, Khomeinishahr, Iran.

<sup>3</sup> Materials and Energy Research Centre, Ceramics Research Institute, Karaj, Iran.

Received: 22 June 2025 - Accepted: 17 November 2025

## Abstract

This study investigates the combined effects of cold rolling and post-rolling heat treatment on the microstructural evolution and mechanical performance of explosively welded Al/Cu joints. Explosive welding produced a wavy interfacial morphology with localized melted zones and brittle intermetallic compounds (IMCs). Cold rolling significantly altered the interface, reducing wave amplitude, promoting grain refinement, and enhancing dislocation density, which resulted in improved hardness and joint strength. Subsequent annealing facilitated recovery and recrystallization in the base metals while promoting the growth and continuity of interfacial IMCs, leading to a dual effect: softening of the bulk layers and localized hardening of the interface. Microhardness testing revealed increased hardness near the bonding line in both as-welded and rolled samples, with the copper layer exhibiting a stronger hardening response due to its lower stacking fault energy. Macro-mechanical testing confirmed that rolling enhanced joint strength, whereas prolonged annealing led to excessive IMC growth and reduced ductility. The optimum balance between strength and ductility was achieved at ~45% thickness reduction combined with carefully controlled annealing conditions.

**Keywords:** EXW, Al/Cu Bimetallic Joints, Cold Rolling, Post-Rolling Heat Treatment, Mechanical Properties.

## 1. Introduction

In recent years, high-performance industries such as aerospace, automotive, power electronics, and heat exchangers have demanded multifunctional, lightweight, and durable materials [1]. Among the most promising approaches is the fabrication of multilayer metal systems by joining dissimilar metals such as copper and aluminum. These metals offer complementary properties due to significant differences in physical characteristics such as density, electrical conductivity, melting point, and stacking fault energy, making their combination highly desirable for functional applications [2,3].

Explosive welding, a solid-state bonding technique, has emerged as a powerful solution for joining dissimilar metals. It utilizes high-velocity impact induced by controlled detonation to form a metallurgical bond between two metal sheets, typically resulting in a wavy or planar interfacial morphology [4,5]. In the Cu–Al system, EXW can lead to the formation of intermetallic compounds (IMCs) such as Al<sub>2</sub>Cu and Al<sub>3</sub>Cu at the interface, which are known for their brittleness and adverse effects on joint toughness [6,7]. To enhance the performance of explosively welded joints, cold rolling is frequently applied as a post-weld deformation process. It improves joint integrity by increasing dislocation density, reducing wave amplitude, and homogenizing the microstructure [8].

Several studies have reported increased hardness and mechanical strength after rolling due to work hardening and grain refinement effects [9,10]. However, excessive deformation may result in damage to the interfacial region or lead to delamination [11].

Furthermore, post-rolling heat treatment (typically annealing) has been proposed to mitigate residual stresses, enable recrystallization, and enhance ductility. This process can also limit the growth of brittle IMCs and refine their morphology [12]. Experimental studies have shown that annealing after rolling significantly improves the tensile strength and toughness of Cu–Al explosive joints [13,16].

Despite extensive investigations on EXW and post-weld rolling, there remains a significant gap in understanding the combined effect of rolling and post-rolling heat treatment on the interfacial structure, IMC formation, microhardness distribution, and mechanical performance of Cu–Al joints.

The present study aims to systematically investigate the combined effects of cold rolling and post-rolling annealing on the metallurgical and mechanical properties of explosively welded Cu–Al joints.

The research focuses on interfacial morphology, IMC evolution, microhardness gradients, and overall joint performance, with the goal of optimizing post-weld processing for industrial applications.

\*Corresponding author

Email address: Khanzadeh@iau.ac.ir

## 2. Materials and Methods

In this study, commercially pure copper sheets ( $250 \times 250 \times 1.5$  mm) and 1000-series aluminum sheets ( $250 \times 250 \times 4.5$  mm) were used as flyer and base plates, respectively, for EXW. Their chemical compositions are listed in Table. 1.

The EXW process was performed using a parallel plate configuration, as shown in Fig. 1.(a). A standoff distance of 3 mm was maintained between the aluminum and copper plates using copper wire spacers. The explosive material used was Amatol 95.5, consisting of 95% ammonium nitrate and 5% trinitrotoluene (TNT), with a particle size of approximately  $8 \mu\text{m}$ . The detonation velocity was measured at 2900 m/s, and an M8 detonator was used for ignition. The explosive was housed in a wooden MDF box with a thickness precisely matching the required explosive layer to ensure uniform energy distribution during detonation.

The main welding parameters including explosive thickness, standoff distance, and the explosive-to-flyer load ratio are summarized in Table. 2.

Following successful welding, the bonded specimens were subjected to cold rolling using a two-high rolling mill equipped with rollers of 150 mm diameter operating at 150 rpm. The rolling was conducted at ambient temperature and without any lubricant. Thickness reductions of 30%, 45%, and 60% were applied to evaluate the effect of strain on the interface morphology and mechanical behavior of the joints. All processing conditions, including rolling and post-weld heat treatment, are consolidated in Table. 2.

Subsequently, selected welded and rolled samples were annealed to assess the effect of post-rolling heat treatment. The annealing treatments were conducted at controlled temperatures and times according to the diagram in Fig. 1. The sample categories used were:

- **EWS:** Explosive Welded Sample (no rolling or heat treatment)
- **H-BR:** Heat-treated Before Rolling
- **H-AR:** Heat-treated After Rolling

Samples of  $10 \times 10$  mm were extracted from each category. After wire-cutting and mounting, the samples were prepared for metallography according to standard grinding and polishing procedures described in ASTM E3 [17] (SiC papers: 60–2500 grit, alumina suspension), cleaned with alcohol, and etched following ASTM E407 using a glycerol–HCl solution [18].

Microstructural characterization was performed using an Olympus BX51M optical microscope at various magnifications. Morphology of the bonding interface, IMC formation, and crack propagation were examined in detail.

Vickers microhardness testing was carried out using a KOOPA MH1 microhardness tester under a load of 50 g and a dwell time of 10 s. Measurements were made along the interfacial thickness at regular intervals. The average of three indentations at each location was recorded. All tests were performed at room temperature ( $25^\circ\text{C}$ ) in accordance with ASTM E384-11 [19].

**Table. 1. Chemical composition of the aluminum and copper plates (wt.%).**

Material / Element	Ti	Cr	Mn	Mg	Si	Zn	P	Pb	Sn	Cu	Al
Aluminum	0.150	0.250	0.700	4.750	0.400	0.250	–	–	0.020	0.020	Bal.
Copper	–	–	–	–	0.119	0.089	0.012	–	0.920	Bal	–

**Table. 2. Process conditions of the tested samples, including EXW, cold rolling, and heat treatment parameters.**

Sample	Explosive Thickness (mm)	Standoff Distance (mm)	Rolling Temp ( $^\circ\text{C}$ )	Thickness Reduction (%)	Heat Treatment Temp ( $^\circ\text{C}$ )	Heat Treatment Time (h)
EWS	13	3	25	–	–	–
H-BR	13	3	–	–	400	1.5
H-AR	13	3	25	60	400	2–6

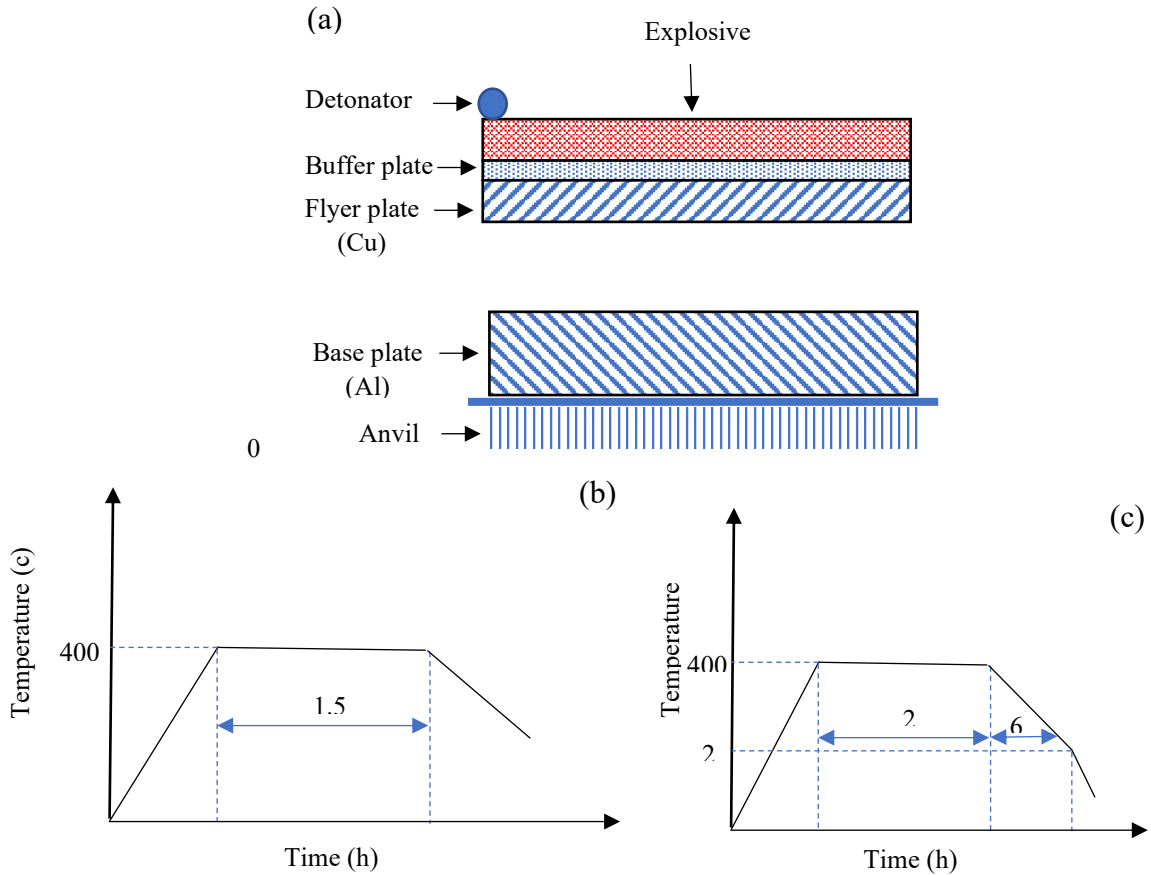


**Fig. 1.** Experimental configuration and heat treatment cycles of the samples: (a) Initial setup of copper and aluminum plates for EXW using parallel configuration; (b) Time–temperature diagram of heat treatment applied before rolling (H-BR); (c) Time–temperature diagram of heat treatment applied after cold rolling (H-AR).

### 3. Result and Discussion

#### 3.1. Microstructure of the As-Welded Explosive Joint

The initial Cu–Al explosive-welded interface (Fig. 2) exhibits the characteristic wavy morphology induced by high-velocity impact, severe plastic deformation, vortex flow, and localized melting. Such morphology, described similarly by Paul et al. [20], indicates strong metallurgical bonding yet raises concern for brittle IMC formation.

The microstructural examination of the Al/Cu explosive weld revealed that the interface exhibited characteristic wavy morphologies generated by the high-velocity impact (Fig. 3). Compared with the as-welded sample (Fig. 2), the H-BR condition exhibited a thicker interfacial IMC layer and higher defect density, primarily due to accelerated diffusion and plastic deformation during rolling [20]. Near the interface, both Al and Cu grains were heavily elongated. This elongation indicates intensive plastic flow and significant strain hardening caused by the high strain-rate deformation.

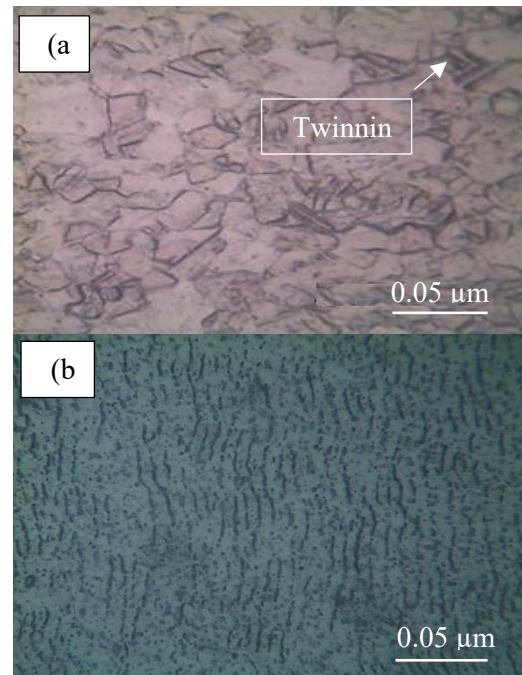


**Fig. 2.** Optical microstructure of the base metals after EXW: (a) copper, (b) aluminum.

Furthermore, the results demonstrated that because of the large density and physical property mismatch between copper and aluminum, the interfacial waves did not form as perfect sinusoidal patterns; the wave amplitude was smaller than the wavelength. With increasing collision energy, plastic deformation intensified, leading to higher wave amplitudes, vortex formation, and localized melting. These effects promoted the nucleation of brittle Al–Cu IMCS as well as adiabatic shear bands, which in some cases acted as preferential sites for microcracks within the interface.

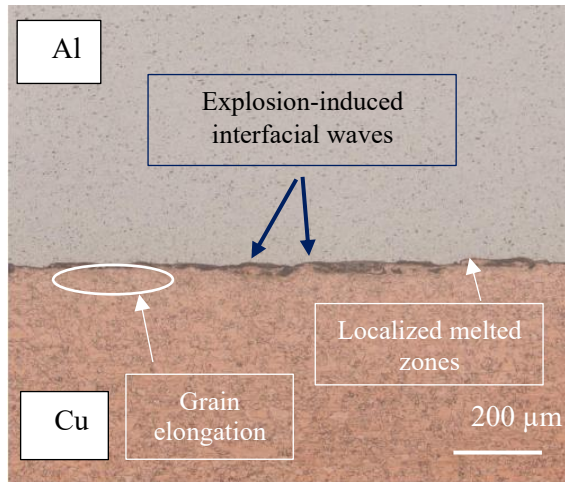


**Fig. 3. Optical microstructure of the Al/Cu joint produced by EXW.**

### 3.2. Effect of Cold Rolling on Interfacial Morphology

The microstructural analysis of the H-BR sample (heat-treated before rolling) revealed significant modifications in the fusion zone and interface after preheating at 400 °C for 1.5 h (Fig. 4). These changes were mainly attributed to two factors: (i) interdiffusion of copper and aluminum due to the increased temperature and concentration gradient, and (ii) enhanced plastic deformation induced by rolling. Preheating also activated additional slip systems, which promoted more intense plastic flow during rolling compared to the non-heated condition. A comparison of the interfacial layer before and after rolling demonstrated a noticeable increase in the thickness of the intermetallic zone. This effect was primarily caused by grain refinement, which increased the density of grain boundaries and accelerated grain boundary diffusion. In addition, the higher density of defects such as dislocations and vacancies facilitated pipe diffusion along dislocation cores, which requires lower activation energy. Consequently, the combined influence of preheating and rolling accelerated diffusion kinetics and promoted faster growth of intermetallic layers at the interface [21].

The microstructural analysis of the H-AR sample (heat-treated after rolling at 400 °C for 6 h) revealed that the interfacial wavy–vortex morphology remained stable following heat treatment (Fig. 5). This geometry is considered favorable in EXW because it provides a larger interfacial area and superior bonding strength compared to flat or continuously melted interfaces. Unlike the as-welded condition,

fewer localized melted zones were observed after heat treatment. This reduction was associated with recovery, recrystallization, and grain growth phenomena, which alleviated shock-induced strain and led to grain coarsening near the interface [20, 21]. Post-rolling heat treatment also promoted atomic diffusion and facilitated the growth of intermetallic layers at the interface. A comparison between the H-BR and H-AR conditions showed that intermetallic thickness increased after heat treatment, whereas the extent of localized melted regions decreased (Fig. 4. and Fig. 5.). In addition, some dark-etched regions appeared at the interface that were absent in the pre-rolled samples.

These features may have originated either from enhanced corrosion susceptibility during etching—caused by higher stored energy and residual melts—or from thickening of the molten layer induced by rolling prior to heat treatment.

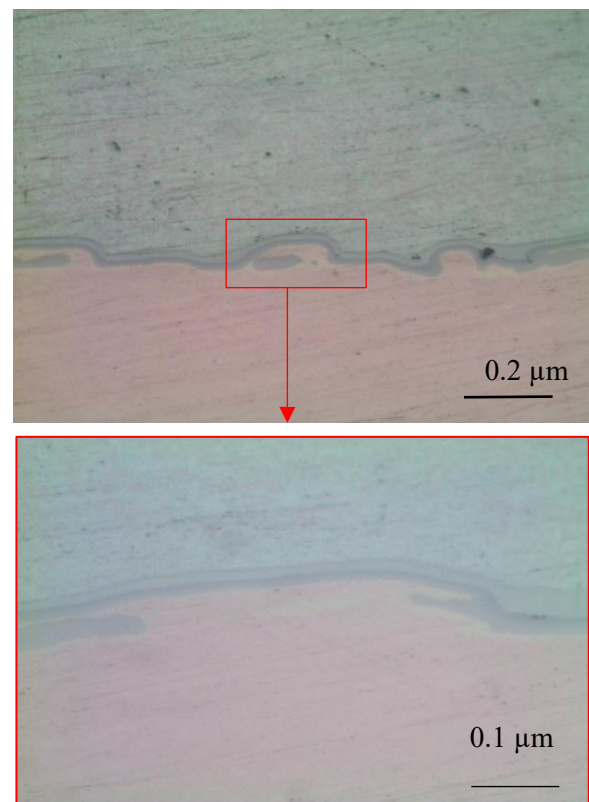


**Fig. 4. Optical microstructure of the Al/Cu explosive weld after heat treatment prior to rolling (H-BR sample).**

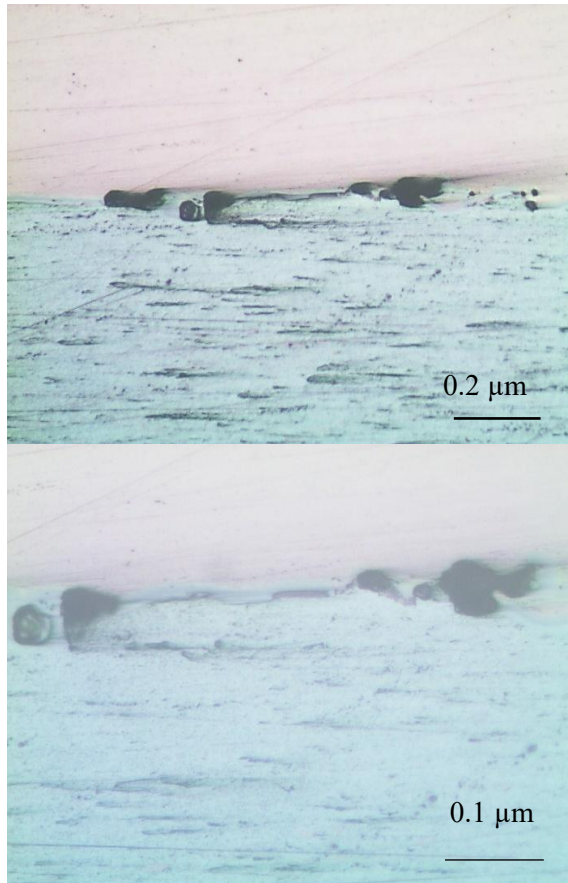


Fig. 5. Optical microstructure of the Al/Cu explosive weld after heat treatment following rolling (H-AR sample). (H-AR) .

### 3.3. Effect of Post-Rolling Annealing

Post-rolling annealing promoted recovery and recrystallization in the Al matrix, while simultaneously facilitating the continuous growth of  $\theta$  ( $\text{Al}_2\text{Cu}$ ) and  $\eta$  ( $\text{AlCu}$ ) IMCs, which may embrittle the interface if excessive (Fig. 6. and Fig. 7.). Kim et al. [22] observed analogous behavior in Cu–Al–Cu strips, where annealing above 350 °C catalyzed formation of continuous IMC layers MDPI. Excessive IMC growth, however, risks embrittlement at the interface.

The microstructure of the Al–Cu joint after 60% thickness reduction is presented in Fig. 7 (a). Compared to the as-welded sample, a significant decrease in wave amplitude and a flattening of vortices are evident.

This effect is directly attributed to the compressive stresses induced during rolling.

The smoothing of vortices and mechanical interlocking created by the rolling process have been reported by several researchers [13,14] as mechanisms that can enhance the interfacial bond strength in EXW.

Additionally, dark regions appeared along the interface, which were less pronounced before rolling.

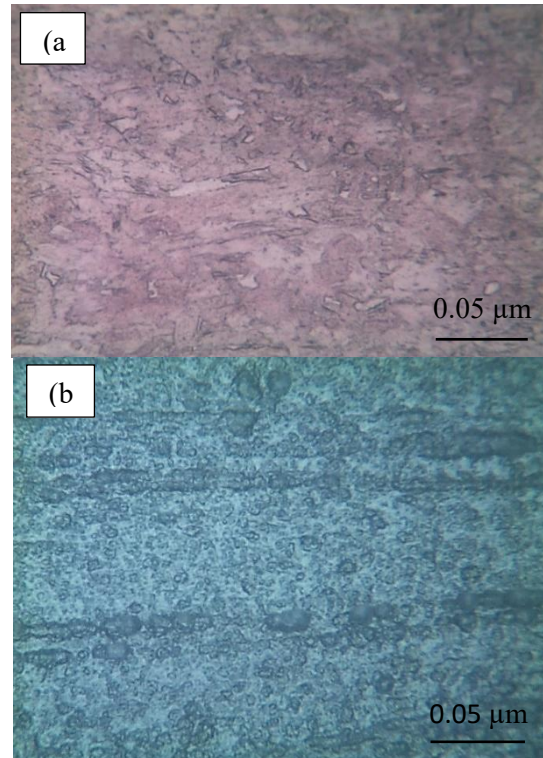


Fig. 6. Optical microstructure of the base metals after EXW and subsequent rolling: (a) copper, (b) aluminum.

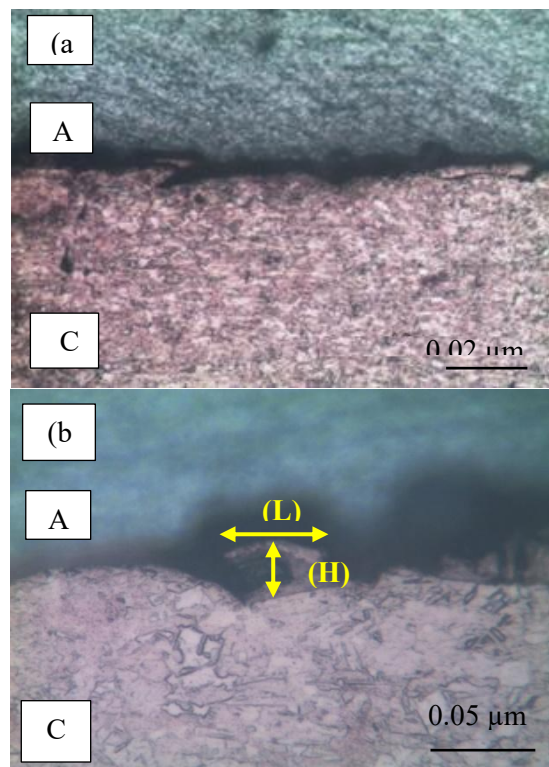


Fig. 7. (a) Optical microstructure of the Al/Cu explosive weld interface after 60% thickness reduction during rolling, shown at two different magnifications. (b) Variation of wavelength and wave amplitude at the Al/Cu interface after rolling with 60% thickness reduction.

They may have resulted from higher susceptibility to etching (due to elevated stored energy in melted regions) or from thickening of the molten layer during rolling. As illustrated in Fig. 7 (b), the wavelength and amplitude of the interface waves decreased with rolling, confirming that the irregularities generated during EXW are progressively flattened under rolling pressure. Similar structural modifications have been widely reported in other severe plastic deformation (SPD) techniques, such as ECAP, ARB, and ECAR, where grain refinement and improved mechanical properties are achieved [15].

### 3.4. Microhardness Analysis of the Al/Cu Joint: As-Welded and Post-Rolled Conditions

Fig. 8 illustrates the microhardness profiles of explosively welded Al/Cu joints for H-BR and H-AR samples. As shown in Fig. 8, hardness increased toward the interface, reaching a maximum within  $\sim 200 \mu\text{m}$ . After rolling (Fig. 9), copper exhibited a stronger hardening response than aluminum due to its lower stacking fault energy, which facilitates dislocation accumulation. As the distance from the interface increases, hardness gradually decreases due to the reduced plastic strain. This behavior is consistent with earlier findings reporting hardness elevation near the bonding zone of explosive welds [23].

Maximum hardness values were recorded within  $\sim 200 \mu\text{m}$  of the interface. The copper layer displayed greater hardening compared with aluminum, which is explained by the lower stacking fault energy of copper ( $78 \text{ mJ/m}^2$ ) relative to aluminum ( $166 \text{ mJ/m}^2$ ). This promotes higher dislocation density in copper, leading to a more pronounced hardness increment. Additionally, surface layers of both metals exhibited higher hardness than their bulk, mainly due to frictional effects and intensified strain near the collision front. However, annealing at  $400^\circ\text{C}$  for 6 h significantly reduced hardness in both layers as a result of recrystallization. The intense plastic deformation near the bonding interface lowers the recrystallization temperature of copper, enabling recrystallization even under relatively moderate heat treatment conditions [24].

Fig. 9. compares microhardness profiles of as-welded and rolled Al/Cu joints. Rolling induced a further increase in hardness across the joint, stemming from uniform plastic deformation throughout the thickness and enhanced strain hardening. The effect was most pronounced in the copper layer near the interface, where hardness rose from  $78.4 \text{ HV}$  to  $106 \text{ HV}$  following a 60% thickness reduction. In contrast, aluminum hardness exhibited a minor increase from  $51.4 \text{ HV}$  to  $52.1 \text{ HV}$ . The stronger hardening response of copper can be linked to its higher kinetic energy absorption during impact and lower stacking

fault energy, which facilitates dislocation accumulation.

The observed trends align with reports by Xu et al. [24], who demonstrated that hardness enhancement in rolled materials is governed by grain refinement and increased dislocation density. In magnesium alloys, they observed a  $\sim 25\%$  hardness increases after the second rolling pass, reaching a maximum improvement of  $\sim 53\%$  by the eighth pass before recovery effects reduced the hardening rate. In the present study, the hardness increment after rolling is similarly attributed to the proliferation of dislocations and deformation twins in both aluminium and copper lattices, induced by the high strain of the rolling process.

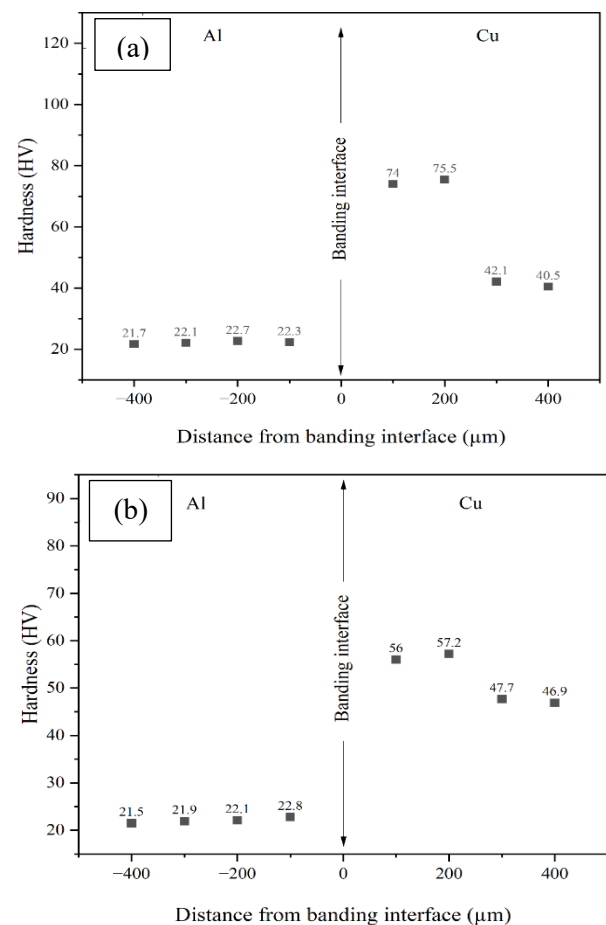


**Fig. 8. Microhardness profiles of the Al/Cu explosive weld: (a) H-BR sample, (b) H-AR sample.**

### 3.5. Effect of Post-Rolling Heat Treatment

Hardness measurements after annealing (Figs. 8–9) confirmed a dual effect: softening of the Cu and Al layers due to recovery/recrystallization, and localized hardening at the interface caused by IMC growth. This trend agrees with previous observations on Cu/Al laminates [22]. This dual effect softening of the base metals and hardening of the interfacial

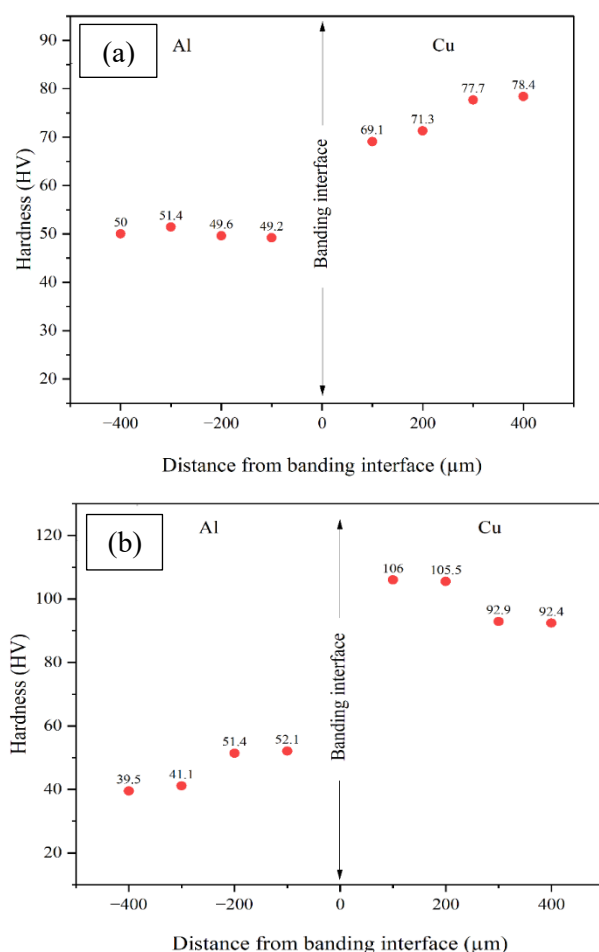


**Fig. 9. Microhardness profiles of the Al/Cu explosive weld: (a) as-welded sample, (b) welded sample after rolling.**

region was also reported by Kim et al. [22] in Cu/Al/Cu layered composites. Nevertheless, excessive IMC growth may result in brittleness and crack initiation.

A comparison of Figs. 8 and 9 further indicates that while rolling substantially increased the overall hardness, subsequent annealing reduced this effect by softening the bulk Cu and Al layers. Nevertheless, localized hardening at the interface persisted after annealing, suggesting that IMC growth dominates hardness behavior at the bonding line under thermal exposure.

### 3.6. Macro-Mechanical Properties

Shear and tensile test results confirmed that rolling enhanced the overall joint strength. This improvement is attributed to an increase in the effective bonding area and the promotion of secondary bonding. However, post-rolling annealing, while improving metallurgical bonding, caused a decline in ductility and toughness when prolonged annealing led to excessive growth of brittle Al–Cu intermetallics. Similar observations were reported by Song et al. [25] for multilayer Al–Cu laminates.

## 4. Conclusion

This study investigated the effects of cold rolling and subsequent heat treatment on the microstructure and mechanical properties of explosive-welded Cu–Al joints. The main findings can be summarized as follows:

1. The as-welded interface exhibited a wavy morphology with vortex flows and localized melted zones, providing strong metallurgical bonding but also promoting the formation of brittle IMCs.
2. Cold rolling flattened the interfacial waves and, at higher reductions ( $\approx 45$ – $60\%$ ), resulted in nearly planar interfaces. Fragmentation of IMCs enabled the formation of secondary bonds within interfacial grooves.
3. Microhardness tests revealed increased hardness at the interface after rolling due to work hardening, whereas post-rolling annealing led to a dual effect: softening of the base metals (recovery/recrystallization) and localized hardening of the interface (IMC growth).
4. Macro-mechanical properties confirmed that rolling enhanced joint strength and bonding continuity. However, prolonged annealing promoted excessive growth of Al–Cu IMCs, causing embrittlement and reduced toughness.
5. The optimum balance between strength and ductility was achieved at  $\sim 45\%$  thickness reduction combined with carefully controlled annealing conditions.

These findings provide practical guidelines for optimizing multilayered Al–Cu laminates used in aerospace structures, electronic packaging, and heat exchanger applications, where both high strength and thermal stability are required.

## References

- [1] Nazeri J, Khanzadeh MR, Bakhtiari H, Seyedraoufi ZS. Investigating the effect of explosive welding variables on the corrosion behavior of copper–aluminum–copper in the salt environment. *Surf Eng Appl Electrochem.* 2024;60(5):698–705.
- [2] Sherpa BB, Saravanan S. Review of the weldability window in explosive welding processes. *J Alloys Metall Syst.* 2024;100150.
- [3] Shiran MRKG, Bakhtiari H, Mousavi SAAA, Khalaj G, Mirhashemi SM. Effect of stand-off distance on the mechanical and metallurgical properties of explosively bonded 321 austenitic stainless steel–1230 aluminum alloy tubes. *Mater Res.* 2017;20(2):291–302.
- [4] Galvão I, Carvalho GHSFL, Pimenta J, Abreu T, Leitão C, Leal RM, Mendes R. Structural analysis of aluminum–titanium–stainless steel three-layer composites produced by explosive welding. *Weld World.* 2024;68(11):2911–2925.

- [5] Gao X, Zhang L, Zhang H, Luo Y. Effect of welding parameters on microstructure and mechanical properties of dissimilar aluminum joints. *J Mater Process Technol.* 2024; 319:117167.
- [6] Shi W, Wang Y, Bi CL, Xu H, Zheng YF, Li B, Xie B. Microstructure and properties of interlocking Cu/Al bimetallic composites by porous lattice additive combined with vacuum liquid infiltration. *J Alloys Compd.* 2025;181142.
- [7] Shiran MKG, Khalaj G, Pouraliakbar H, Jandaghi MR, Dehnavi AS, Bakhtiari H. Multilayer Cu/Al/Cu explosive welded joints: characterizing heat treatment effect on interface microstructure and mechanical properties. *J Manuf Process.* 2018; 35:657–663.
- [8] Paul H, Lityńska-Dobrzyńska L, Miszczyk M, Prażmowski M. Microstructure and phase transformations near the bonding zone of Al/Cu clad manufactured by explosive welding. *Arch Metall Mater.* 2012;57(4):1151–1162.
- [9] Asemabadi M, Sedighi M, Honarpisheh M. Investigation of cold rolling influence on the mechanical properties of explosive-welded Al/Cu bimetal. *Mater Sci Eng A.* 2012; 558:144–149.
- [10] Loureiro A, Mendes R, Ribeiro JB, Leal RM, Galvão I. Effect of explosive mixture on quality of explosive welds of copper to aluminium. *Mater Des.* 2016; 95:256–267.
- [11] Hoseini-Athar MM, Tolaminejad B. Interface morphology and mechanical properties of Al–Cu–Al laminated composites fabricated by explosive welding and subsequent rolling process. *Met Mater Int.* 2016;22(4):670–680.
- [12] Khan HA, Asim K, Akram F, Hameed A, Khan A, Mansoor B. Roll bonding processes: state-of-the-art and future perspectives. *Metals.* 2021;11(9):1344.
- [13] Wang WJ, Wang H, Liu XF, Liu ZC. Interface evolution and strengthening of two-step roll bonded copper/aluminum clad composites. *Mater Charact.* 2023; 199:112778.
- [14] Zhang J, Ma L, Zhao G, Cai Z, Zhi C. Effect of annealing temperature on tensile fracture behavior of AZ31/6061 explosive composite plate. *J Mater Res Technol.* 2022; 19:4325–4336.
- [15] Tayyebi M, Rahmatabadi D, Karimi A, Adhami M, Hashemi R. Investigation of annealing treatment on interfacial and mechanical properties of Al5052/Cu multilayered composites subjected to ARB process. *J Alloys Compd.* 2021; 871:159513.
- [16] Bakhtiari H, Abbasi H, Sabet H, Khanzadeh MR, Farvizi M. Investigation on the effects of explosive welding parameters on the mechanical properties and electrical conductivity of Al–Cu bimetal. *J Environ Friendly Mater.* 2022;6(2):31–37.
- [17] ASTM International. ASTM E3-11(2022), Standard Guide for Preparation of Metallographic Specimens. West Conshohocken, PA: ASTM International; 2022.
- [18] ASTM International. ASTM E407-20, Standard Practice for Microetching Metals and Alloys. West Conshohocken, PA: ASTM International; 2020.
- [19] ASTM International. ASTM E384-17, Standard test method for micro-indentation hardness of materials. West Conshohocken, PA: ASTM International; 2017.
- [20] Paul H, Skuza W, Chulist R, Miszczyk M, Gałka A, Prażmowski M, Pstruś J. Effect of interface morphology on electro-mechanical properties of Ti/Cu clad composites produced by explosive welding. *Metall Mater Trans A.* 2020;51(2):750–766.
- [21] Lee SH, Kim YK, Lee DJ. Microstructural evolution and mechanical properties of roll-bonded copper/aluminum laminates. *Mater Sci Eng A.* 2023; 871:144905.
- [22] Kim YK, Hong SI. Effect of intermetallic compound layer on peel strength and crack propagation behavior in Cu/Al/Cu clad composites. *Metals.* 2019;9(11):1155.
- [23] Zhou Q, Liu R, Ran C, Fan K, Xie J, Chen P. Effect of microstructure on mechanical properties of titanium–steel explosive welding interface. *Mater Sci Eng A.* 2022; 830:142260.
- [24] Xu J, Li C, Wang L, Zhang Y, Chen X. Effect of cold rolling and annealing on interfacial microstructure and properties of Al–Cu explosive welds. *J Mater Res Technol.* 2022; 18:1329–1342.
- [25] Song J, Han P, Li C, Zhang J. Mechanical behavior and fracture mechanisms of multilayered Al–Cu laminates. *Mater Sci Eng A.* 2018; 728:172–182.